

Processes of Replacement by Melt at Interaction between Refractory Materials and Industrially Produced Melts

E. N. Gramenitskiy^{a, *}, T. I. Shchekina^{a, **}, and Ya. O. Alferyeva^{a, ***}

^aGeological Faculty, Moscow State University, Moscow, 119991 Russia

*e-mail: engramen@geol.msu.ru

**e-mail: t-shchekina@mail.ru

***e-mail: yanaalf@ya.ru

Received October 19, 2017; in final form, December 21, 2017

Abstract—In a number of industries (ferrous and nonferrous metallurgy, glass-making and silicate-producing technologies), interaction between refractory materials with melts results in sequences of reaction zonation (reaction columns) that show all principal features of diffusion-controlled metasomatic zoning. However, in contrast to the latter, reaction melt is generated together with crystalline phases in the rear zones of the columns. This melt is neither mechanically displaced melt that affects the refractory materials, nor produced by melting. The process generating this melt is most adequately defined as *replacement by melt*. The principal characteristics of the zoning are discussed below with reference to the corrosion of chromite–periclase refractory materials with melted slag in nickel-producing metallurgy. Similarities between the relations observed under different conditions and in different systems and the evolutionary dynamics of the process, specifics of melt generation and changes in its composition in the zones are demonstrated below with the use of data on other technologies and their experimental modeling. The mechanism of melt replacement is applicable to describing natural reaction processes of magma interaction with host rocks (magmatic replacement), with the following unobvious implications. (1) It is reasonable to expect that the minerals of the rocks should host melt inclusions. (2) It is reasonable to expect that certain minerals should be found in two distinct populations: (i) those in equilibrium with melt in the reaction column and (ii) those crystallizing from the cooling melt. (3) Two or more zones of the column can consist of the same minerals, but their proportions should be different. (4) Plastic deformations in the rear zones of the column (magmatic replacement) should be associated with brittle ones in the pristine host rocks and frontal (metasomatic) zones. (5) In contrast to the rocks of metasomatic columns, the material of magmatic-replacement zones can flow through fractures cutting across the host metasomatic rocks and thereby intersect the outer metasomatic zones.

Keywords: melt (magmatic) replacement, reaction columns, diffusion, corrosion of refractory materials, melted slag, ferrous and nonferrous metallurgy, glass industry

DOI: 10.1134/S0869591118040033

INTRODUCTION

Mechanisms of interaction between melts and compositionally contrasting crystalline rocks (or artificial materials) with the development of reaction zoning were studied by the authors and published in our earlier papers in 1983–2005 (see references and references therein). We are not aware of any analogous concepts published by other researchers. We view our concepts and hypotheses as the development of D.S. Korzhinskii's (1952) hypothesis of granitization as magmatic replacement. As mentioned in his papers, the processes should be associated with the development of zoning in the rocks. We have used implications of D.S. Korzhinskii's (1982) theory of metasomatism and attempted to apply them more broadly, for example, to reaction processes involving melts.

In addition to granitization (migmatization), reactions between natural melts and crystalline rocks occur when host rocks are assimilated by magma (and the magma is thereby contaminated with these rocks). As a whole, the process encompassing not only changes in the melt but also in the host crystalline rocks was referred to as *diffusion-controlled magmatic replacement* in the national literature (Zharikov, 1969) and as *cross-assimilation* in the literature in English (*Glossary of Geology*, 1974).

A schematic graphical representation of the process is offered in Fig. 1 with reference to interaction between leucocratic granite (point 1) and a mafic host rock (point 2) under amphibolite-facies P – T parameters. At given P – T parameters, the two parts of the system occur in different states: subsolidus for one of them and liquidus for the other. At contact between

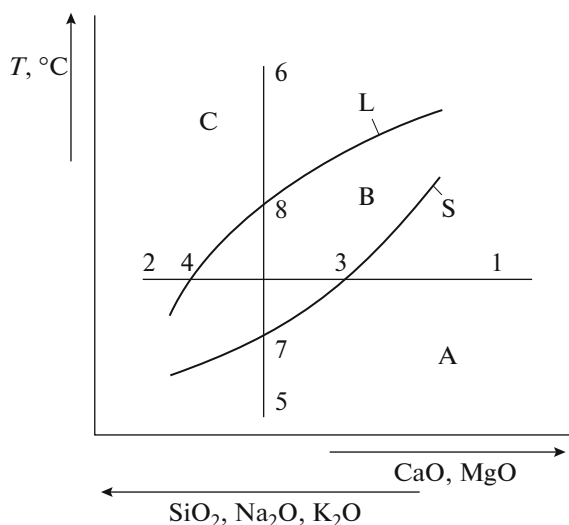


Fig. 1. Schematic representation of differences between magmatic (melt) replacement (horizontal line 1 → 3 → 4 → 2) from melting (vertical line 5 → 7 → 8 → 6). L and S are the liquidus and solidus lines, respectively, and A, B, and C are, respectively, the subsolidus, subliquidus, and liquidus regions.

them, gradients of the chemical potentials trigger diffusion of components. The reaction zoning produced thereby reflects a succession of isothermal phase transitions caused by changes in the chemical composition of the system: the addition or removal of components. In the crystalline rock, the gradient zone begins in the subsolidus region (between points 1 and 3), and the developing zoning is metasomatic. The transition to the subliquidus region (point 3) is associated with the origin of melt, and across this region (from point 3 to point 4), with the increase of amount of melt and conversely, decrease of the total content and number of the crystalline phases. This process seems to be similar, in a sense, to isochemical melting (5 → 7 → 8 → 6), but is, at the same time, notably different from it, as is evident upon its closer examination. First, melt is generated due to a change in the composition of the system (point 3) but not a temperature increase. Second, the compositional trends of the melt and crystalline phases are different during melting and magmatic replacement, and moreover, are often opposite.

The development of zoning in nature according to this mechanism was confirmed by direct experimental modeling of this process as a diffusion- (Gramenitskiy et al., 2002) and infiltration-controlled (Khodorevskaya et al., 2003) ones and by modeling some of the equilibria (Gramenitskiy and Lunin, 1996).

The origin of reaction rims at contacts between melts and refractory materials leads to the corrosion of the latter and their destruction and has long been known in pyrometallurgy, the glass-making industry, and other high-temperature technologies. Our studies over the two past decades have shown that chemical

interaction with the origin of partly molten zones is the main wear and destruction factor of refractory materials. This process is facilitated by two others: the erosion of the refractory materials by moving melt and thermal impact on them.

Although the chemical compositions of the systems and newly formed phases are remarkably different, as also are the parameters of the processes in nature and in various industries, the processes of melt (magmatic) replacement and the development of zoning are similar in their core meaning. The parameters of the technological processes (and experimental modeling) are known, and their interpretations are more obvious than those of analogous processes in nature. In this publication, interaction between refractory materials and industrially generated melts is analyzed to gain an insight into the general relations and trends of such processes, which are, we hope, of much interest for geologists. To do this, we employ materials presented in the quoted publications, which were devoted mostly to the solution of applied problems.

Our experience of communications with our colleagues has shown that the concepts are difficult to understand largely because certain terms are used in unusual contexts. These are:

- (1) metasomatism is one of replacement processes;
- (2) melt (magmatic) replacement is not a melting process;
- (3) analysis of phase equilibria involves not only minerals but also other phases, regardless of their state, and melts should thereby be regarded as analogues with minerals of variable composition;
- (4) by analogy to similar features of diffusion-controlled metasomatism, the development of the zoning is regarded as a result of efficient diffusion-driven interaction between two compositionally contrasting materials.

The authors do not claim to suggest a comprehensive theory of the process, and this publication almost does not discuss the actual phases that transport material or the kinetics of the interaction that are not immediately evident from the facts presented below.

METHODS

The inner structure of the reaction zones is discussed below using examples of studied interaction between refractory materials and melted slags (Table 1): (1) in the pyrometallurgical processes of nickel recovery from sulfide ores; (2) in experimental modeling of these processes; (3) in the process of sulfidization of oxide nickel ores in horizontal metallurgical converter vessels; (4) in steelmaking; and (5) at contacts between refractory materials and glass melt in modeling glass production.

For industrial nickel production by process (1), oxide and sulfide ores are utilized. The technologies always involve a number of stages conducted using

Table 1. Characteristics of industrial processes of interaction between refractory materials and melts and their experimental modeling quoted in this paper

No.	Process*	Refractory material	Melt	T , °C	Gradient T , °C/cm	Buffer
1	Ni smelting from sulfide ores in electric arc furnaces	SL3D	Slag	1600–1700	20–30	NB
2	Modeling of Ni smelting from sulfide ores	SL3D	Slag **	1600	No	NB
3	Ni smelting from oxide ores in converter vessels, sulfidization stage	KhPTU	Slag	1400	15–20	MW
4	Steel making in Martin furnaces	ANKERARTH CP-30; JEHEARTH 33GP	Slag	1500–1600	20–30	IW
5	Modeling of glass-making	KhATs-30	Melted glass **	1500	No	MH
		Bakor-33		1400		

* See the following publications for detailed characteristics of the processes: (1) Shchekina et al., 2011; (2) Shchekina et al., 2014; (3) Gramenitskiy et al., 2005; (4) OJSC Omutninskii Metallurgical Plant, Shchekina et al., 2006a, 2006b; (5) Gramenitskiy and Batanova, 1990. ** The experiments were conducted with type-1 industrial slag and glass made using the quoted brands of refractory materials.

various equipment and facilities. The samples used in this study were produced by smelting Cu–Ni ores in electric arc furnaces. In this technology, the heat source is an alternating-current arc between the electrodes and ore charge, with the temperature in the arc itself sometimes exceeding 2000°C. The product is Cu–Ni matte, which contains 9–13% Ni (in the form of Ni_3S_2), 8–10% Cu (Cu_2S), 48–56% Fe (FeS), and subordinate amounts of Co, PGE, etc.

The altered refractory materials of process (3) are formed during the sulfidization stage when Ni is produced from oxidized ores. Molten matte produced during the previous stage is poured into a converter furnace, into which quartz sand and pyrite are also placed and which is blown with air doses to oxidize the sulfide and to slag the iron. The exothermal oxidation reaction provides heat to counterbalance the heat consumption.

The principle of steel production in Martin furnaces by process (4) is as follows: crude iron and scrap metal are processed on the bottom of a reverberatory air-furnace. The bulk charge (scrap metal) is placed into the furnace and is poured over with liquid crude iron. The temperature required for the process (1500–1600°C) is maintained by burning natural gas. The furnace is heated by burning gas–air mixture fed into the working space through injectors in the end-walls of the working volume.

In all three processes, slag is formed as a layer above the product: the metal, matte, or converter matte. In modeling the process of nickel production, slag was placed in contact with refractory material at the very beginning of the experiment. In metallurgy, slag tapping interrupts the interaction process, but the inertial metallurgical facilities continue to cool for a

few days. In contrast to the industrial process, the experimental runs were rapidly quenched upon terminating.

The refractory materials used in (1), (2), and (3) are chromite–periclase, with various chromite concentrations. In our experimental modeling of the glass-making process (5), the refractory materials consist of mullite with 5–7 wt % ZrO_2 and baddeleyite–corundum bricks. In steel-making technologies (4), magnesite–dolomite powder mixtures are utilized. The refractory materials are affected by melted slag of different composition. They are in equilibrium with immiscible melts of nickel matte (1), nickel (2), nickel matte (3), and iron (4). The highly alkaline molten glass (5) has a principally different composition.

The temperature regime in each of the technological processes was estimated from equilibria in the corresponding systems, including the liquidus and solidus temperatures of the generated melts. The temperature of the melts varied from 1400 to 1700°C, and the temperature gradient across the refractory lining was 15–30°C/cm. In the experiments, the temperature was measured with thermocouples or pyrometers. Both the melt and the refractory material were placed into the gradient-free zone (at temperatures of 1400–1600°C, measured accurate to $\pm 10^\circ\text{C}$).

As follows from the origin of buffer associations, oxygen fugacity was close to the nickel–bunsenite equilibrium during nickel smelting (1) and its modeling (2); to the magnetite–wüstite buffer during sulfidization (3); and to iron–wüstite one during steel making (4). No redox transformations occur during glass melting. Because the process is carried out in contact with atmospheric air, the oxygen partial pressure should be close to 0.2 bar, which corresponds to the

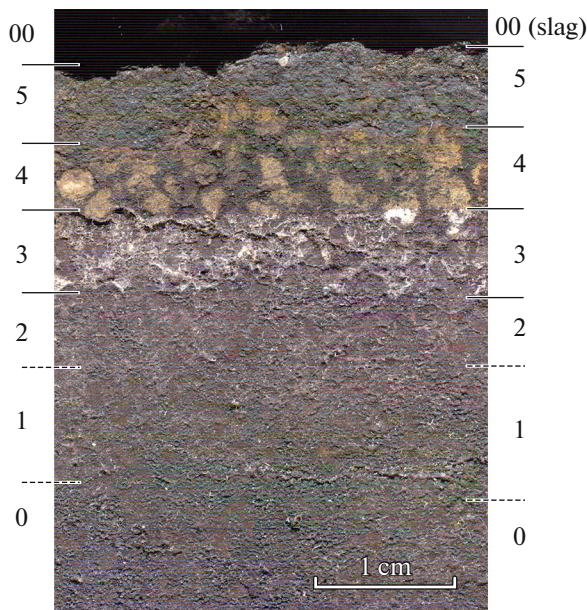


Fig. 2. Photograph of a cross section of firebrick used in nickel-making. Zones 1–5 separate the slag (above zone 5) from unaltered refractory material (zone 0).

hematite stability field at temperatures of 1400–1500°C and is close to the magnetite–hematite buffer.

In all of the examples, a zoned reaction region was formed, which always contained glass in its rear zones, in spite of the significant differences in the parameters of the processes and in the composition of the reacting materials. As a basic reference example, we analyzed the column produced when refractory material interacted with melted slag in the process of nickel smelting in arc furnaces. Certain features of the zoning, for example, the contamination of the melt coupled with changes in the refractory material, the composition of the melt, its changes near the refractory material, and the possibility of mechanical displacement are discussed with reference to the other examples.

The inner structure of the reaction zones was analyzed based on similarities with metasomatic zones. We have also analyzed the phase and chemical composition of the reaction zones, the character of their boundaries, and changes in cross sections. The inner structure of the zones was examined using optical, electron-microscopic, and X-ray powder diffraction techniques. The chemical composition of all phases was analyzed by a Jeol JSM-6480LV scanning electron microscope equipped with an INCA-Energy 350 energy-dispersive spectrometer at the Department of Petrology of the Moscow State University. The techniques applied to study the composition of the materials are described in much detail in the quoted papers. Much attention was paid to the melts, more specifically, to the glasses and quench crystalline phases produced by these melts. Mineral reactions at zone boundaries were studied by calculating and analyzing

the reaction equations, similar to what is done when metasomatic processes are studied (Gramenitskiy, 2012). The calculation procedures are described below in the sections *Estimation of Melt Composition* and *Generalized Inner Structure of the Column*.

RESULTS

An example of the zoning. In two samples of refractory materials altered in contact with melted slag during nickel smelting in arc furnaces (at the Norilsk Nickel Mining and Metallurgical Company), a column was formed that consisted of five reaction zones. All of the zones are clearly seen in a cross section of the specimen (Fig. 2). The total thickness of all zones and the thicknesses of each of them are greater for the sample from the phase region than that from the inter-phase one, but the number of the zones, the ratios of their thicknesses, their chemical and mineralogical composition, and the phase (minerals and glass) proportions and compositions in each zone are almost identical. This also pertains to the sample obtained by experimental modeling of the process.

The concentrations of all major components, Ni, and Co in the primary materials (the frontal and rear zones) are significantly different (Table 2). Successive reaction zones demonstrate a systematic change of phase and chemical composition, which stepwise approaches the compositions of refractory materials and slags.

The primary refractory material (Table 2, zone 0) consists of periclase, Cr-spinel, and monticellite, which make up 65, 25, and 10 vol % of the rock, respectively. The periclase aggregates are 0.5–2 mm across, compact, and consist of equant grains 0.2 mm in diameter.¹ The brecciated spinel aggregates are composed of grain fragments 0.02–0.1 mm. All of them are cemented by smaller (no larger than a few dozen micrometers) grains of the same minerals. Periclase at the boundaries of the aggregates hosts micrometer-sized inclusions of Cr-free spinel (Fig. 3). The material is massive in structure, and its pores are no larger than 1 mm in diameter.

In zone 1, periclase content decreases (to 50 vol %), and that of spinel slightly increases (30 vol %), and the intergranular space between grains of major minerals contains, along with monticellite, also olivine. In Fig. 2, the transition from zone 0 to zone 1 is discernible mostly in the fabrics of the material: the aggregate texture of the periclase and the clastic one of the spinel gradually disappear and give way to a granoblastic tex-

¹The following symbols and abbreviations are used below: *Bu*—bunsenite, *Cpx*—clinopyroxene, *Mtc*—monticellite, *Ol*—olivine, *Per*—periclase, *Spl*—spinel, *Ws*—wüstite, *Gl*—glass, *L*—melt, *MeL*—phase quenched from metallic melt; oxygen buffers: *IW*—iron-wüstite, *MH*—magnetite–hematite, *MW*—magnetite–wüstite, *NB*—nickel–bunsenite.

Table 2. Composition (wt %) of zones of the column and its phases produced at the corrosion of the refractory material by slag in the process of nickel making in electric furnaces

Component	zone 0		zone 1			zone 2			Olivine			
	Periclase	Spinel	Monticellite	Primary refractory material*	Periclase	Spinel	Monticellite	Olivine		Bulk composition of zone**	Periclase	Spinel
SiO ₂	0.00	0.00	38.47	1.91	0.00	0.00	38.77	41.84	5.94	1.07	0.00	39.97
TiO ₂	0.00	0.00	0.00	0.00	0.00	0.00	0.00	0.00	0.00	0.00	0.00	0.00
Al ₂ O ₃	3.87	14.66	0.00	5.81	2.93	21.64	0.00	0.42	6.20	4.84	17.63	0.00
Cr ₂ O ₃	5.78	57.83	0.00	16.20	8.07	54.57	0.00	0.00	16.00	9.19	52.67	0.00
FeO	10.92	24.42	2.30	10.87	14.00	9.00	2.55	1.75	10.90	11.89	7.50	3.06
MgO	78.94	22.15	26.84	59.73	77.16	17.71	28.11	52.38	57.44	72.97	19.15	50.16
MnO	0.00	0.00	0.00	0.00	0.38	0.00	0.29	0.00	0.26	0.24	0.00	0.21
NiO	0.00	0.00	0.00	0.00	0.00	0.00	0.00	0.00	0.00	0.00	0.00	0.00
CoO	0.00	0.00	0.00	0.00	0.00	0.00	0.00	0.00	0.00	0.00	0.00	0.00
CaO	0.00	0.00	32.31	1.61	0.17	0.00	30.99	3.80	3.12	0.64	0.00	4.60
Na ₂ O	0.00	0.00	0.00	0.00	0.22	0.00	0.00	0.00	0.14	0.38	0.00	0.00
K ₂ O	0.00	0.00	0.00	0.00	0.00	0.00	0.00	0.00	0.00	0.00	0.00	0.00
Total	99.51	100.29	99.92	96.13	102.93	102.92	100.71	100.19	100.00	101.22	96.95	98.00
Component	zone 2		zone 3			zone 4			zone 5			Slag*
	Melt***	Bulk composition of zone**	Periclase	Spinel	Melt***	Bulk composition of zone**	Spinel	Melt***	Bulk composition of zone**	Melt***	Bulk composition of zone**	
SiO ₂	36.11	10.26	0.47	0.00	35.67	10.82	0.00	32.79	27.78	28.08	29.60	44.09
TiO ₂	0.59	0.00	0.00	0.25	0.71	0.00	0.25	0.33	0.43	0.43	0.26	0.75
Al ₂ O ₃	20.22	7.96	8.50	17.71	16.12	8.74	18.27	11.76	10.39	10.54	12.45	15.80
Cr ₂ O ₃	2.72	14.47	2.43	49.71	0.44	13.28	49.18	0.54	5.98	2.03	1.50	0.26
FeO	19.44	12.46	23.67	8.14	17.99	13.79	22.53	24.24	25.46	25.86	24.25	17.10
MgO	2.49	48.86	60.60	19.88	3.48	42.21	8.81	4.41	6.45	6.33	5.26	7.11
MnO	0.64	0.25	0.00	0.00	0.66	0.37	0.00	0.08	0.00	0.00	0.00	0.29
NiO	3.24	0.00	2.16	0.00	8.05	5.50	0.00	13.98	13.88	14.03	15.63	0.99
CoO	1.26	0.00	1.26	0.00	1.65	1.30	0.00	2.11	1.90	2.02	2.12	1.02
CaO	9.39	3.36	0.00	0.00	12.10	3.53	0.00	7.38	4.59	5.22	6.85	9.68
Na ₂ O	2.19	0.32	0.00	0.00	1.76	0.39	0.00	1.02	0.67	0.84	0.84	1.02
K ₂ O	1.72	0.34	0.00	0.00	1.39	0.41	0.00	1.36	0.77	0.81	1.24	0.93
Total	100.00	98.28	99.34	95.69	100.00	103.34	99.04	100.00	98.30	96.19	100.00	99.04

* Chemical compositions of individual samples of the primary refractory material and slag; **microprobe analyses (scanning over an area); ***calculated melt compositions; average of two, by two methods (see Table 5).

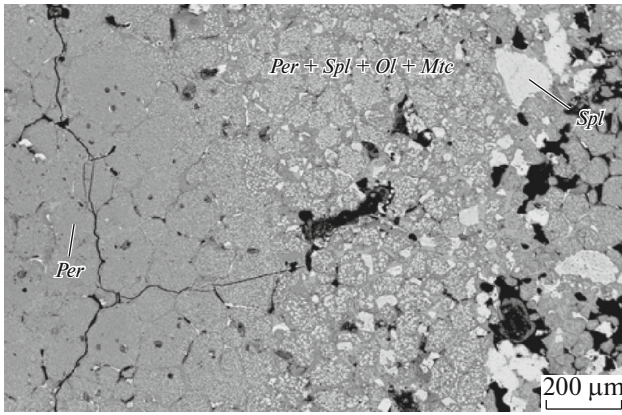


Fig. 3. Typical texture of the primary refractory material. Micrometer-sized ingrowths of Cr-free spinel and monticellite occur at contact between periclase and Cr-spinel. BSE image.

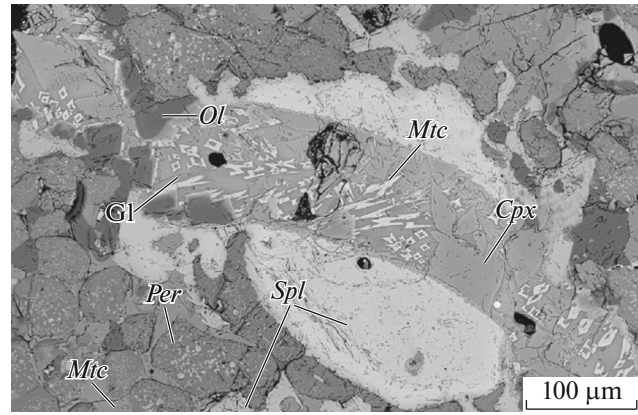


Fig. 4. Glass veinlet hosting clinopyroxene, monticellite, and olivine crystals. The monticellite, olivine, and spinel occur in two populations. BSE image.

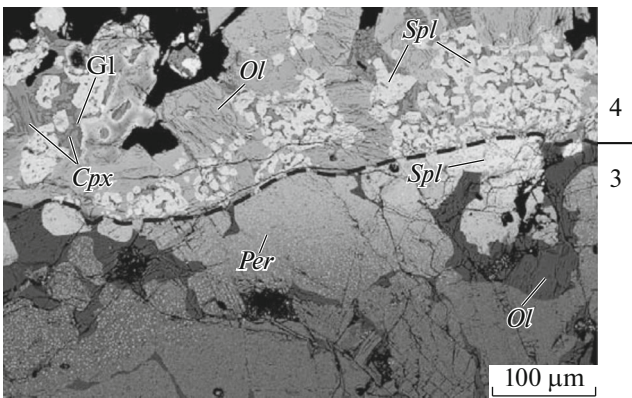


Fig. 5. Sharply defined in phase composition and texture at the boundary of zones 3 and 4 (dashed line) and the appearance of vermicular glass segregations in spinel grains. BSE image.

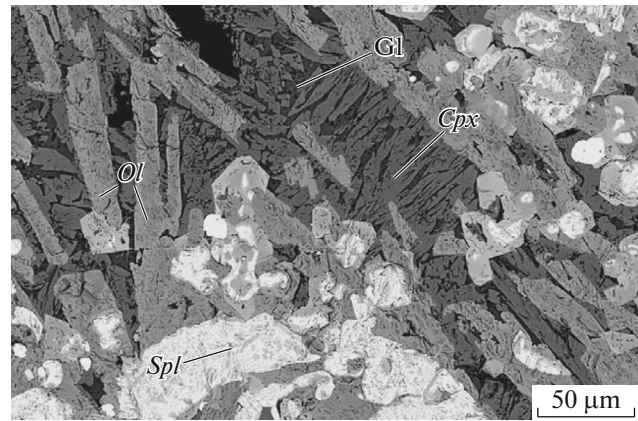


Fig. 6. Texture of zone 4. Crystals of population I are only large anhedral spinel grains. Skeletal clinopyroxene and olivine crystals and small zoned spinel grains are hosted in glass and belong to population II. BSE image.

ture, with grains 0.3–0.7 mm across and with the diameter of the pores increasing to 2 mm.

In the groundmass of the altered refractory material from zone 2, silicate minerals almost completely disappear, and equant, lenticular, and veinlet-shaped segregations of silicate glass (Fig. 4) appear. They host monticellite and clinopyroxene crystals and olivine rims between periclase grains and glass. The quenched melt (glass) and silicates in it make up 15 vol %. The aggregates are usually found in association with relict spinel grains (which are recrystallized and whose composition is modified).

Zone 3 is also dominated by periclase and spinel (up to 35 vol %), but the material is finer grained than in the previous zones. The content of glass veinlets and lenses with skeletal crystals of spinel, clinopyroxene, and other quench minerals notably increases (up to 25 vol %). The amount of pores decreases.

The transition to zone 4 is sharp, with periclase completely disappearing at the boundary. The boundary is contoured by chains of pores a few millimeter in diameter. The pores account for approximately 20 vol % of this zone. The content of glass drastically increases to 65 vol %. The spinel typically hosts worm-shaped glass inclusions a few micrometers long (Fig. 5). Zones 2–4 host spinel grains of two types. Relatively large round individuals often form ring-shaped accumulations (Fig. 6), which were likely inherited from the original texture of the refractory material. Both the smaller euhedral crystals and the elongate skeletal crystals of the silicates (olivine, clinopyroxene, and monticellite) are hosted in glass.

Zone 5 typically has a vitreous texture with numerous bubbles. The olivine forms dendritic crystals, and the clinopyroxene occurs as elongate prismatic ones. Small euhedral grains of Fe-rich spinel and bunsenite are found in subordinate amounts.

The slag (Table 2, zone 00) consists of a light and porous material. The bubbles range from 2 to 30 mm and are separated from one another by porous glass. The glass contains continuous bands of aggregates of dendritic and star-shape clinopyroxene crystals, euhedral spinel crystals, and sometimes also round metal droplets 10–20 μm in diameter.

Phase composition of the zones. Mineral phases of the zones obviously belong to two populations. The earlier phases (which crystallized during reaction interaction) are partly relict and mostly recrystallized, with changes in the composition of the minerals of the original refractory material of previous zone. Their composition is reported in Table 2. The phases of the later population (which crystallized during cooling) are the quench melt and its crystallization products (Table 3). The minerals of both populations are compositionally heterogeneous (zoned).

Periclase is found in the original refractory material (zone 0) and in the frontal zones (1–3) of the reaction column, in which periclase grains are recrystallized, expel solid inclusions, but obviously inherit their setting from the textural pattern of the original refractory material. Iron concentration in the mineral is negatively correlated with the Mg concentration and systematically increases to 0.21 a.p.f.u. from zone 0 to zone 3 (Fig. 7). Up to zone 2, Ni concentration in the periclase is below the detection limit and gradually increases in zone 3 to 0.33 a.p.f.u., and the mineral contains admixtures of Co and Cu (along with Ni): up to 0.03 a.p.f.u. Bunsenite (herein we understand it as oxides with a mole fraction of $\text{NiO} > 0.5$) is found in zones 4 and 5 and is always hosted in glass. In contrast to the periclase, this mineral crystallized from melt.

Minerals of the spinel group are found in all reaction zones, in the primary refractory material, and even in the slag.

In the refractory material, these are angular clastic grains, whose size ranges from a few to 200 μm . In addition, micrometer- and submicrometer-sized magnetite inclusions in periclase were found at the boundary of the clastic aggregates (Fig. 3). They crystallized when the refractory material was produced.

In zones 1, 2, and 3, the clastic angular shapes of spinel grains are smoothed, they acquire poorly pronounced zoning, and the grain size becomes more uniform, 60–80 μm on average. The newly formed granoblastic texture inherits the general textural pattern, with spinel occurring around large periclase aggregates or crystals. Relics of this texture are discernible even in zone 4, which contains no periclase but whose spinel sometimes occurs as grain garlands (Fig. 6). We ascribe these spinel varieties to population I.

In zones 2–5, another morphological variety of spinel is found (its population II), which is spatially constrained to glass segregations: these are euhedral, contrastingly zoned crystals 30–50 μm across (Figs. 5, 6). Some of them have concave crystal faces because of

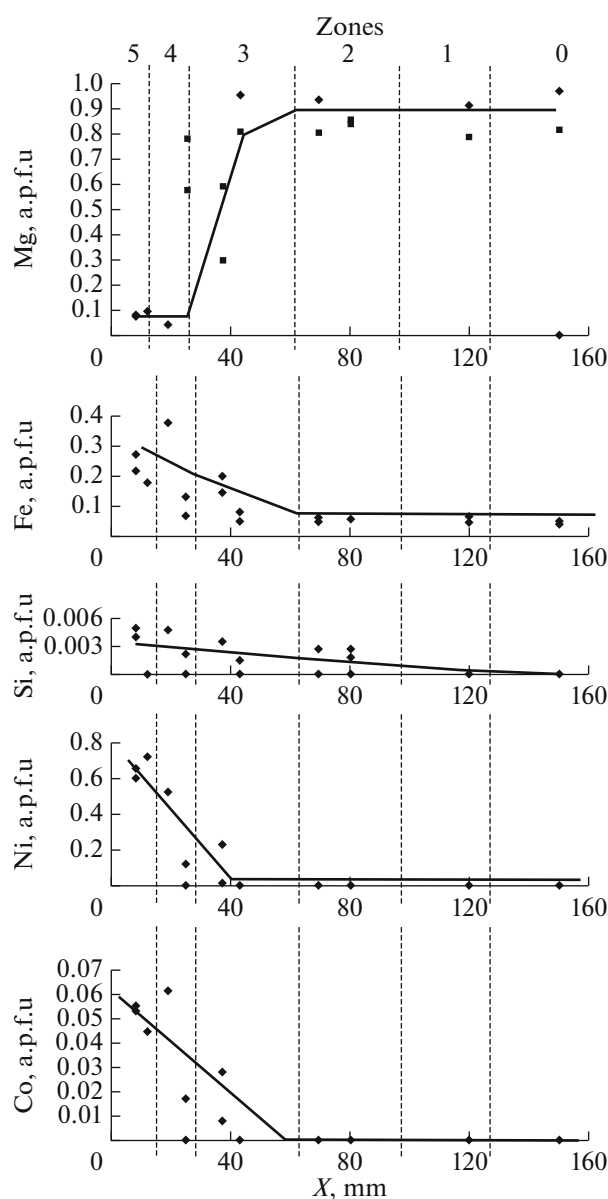


Fig. 7. Systematic variations in the concentrations of major components (in a.p.f.u.) in periclase across the reaction zones in a refractory material sample.

the faster growth of their edges and/or apices. Spinel in the slag shows similar morphologies.

Systematic trends in the composition of the spinel are discernible after its analyses are classified according not only to the zones but also to crystallization stages. The composition of the mineral of population I gradually changes along the column from magnesiochromite in the primary refractory material and the first two zones to Ni-bearing ferrimagnesiochromite in zones 3 and 4. The composition of the cores of the zoned grains is the same as spinel composition in the previous zone. The crystals of population II in zones 2 and 3 correspond to Ni-bearing spinel, and those in

Table 3. Composition (wt %) of quench phases of melt (glass and minerals of population II)

Component	zone 2					zone 3			zone 4	
	Glass	Spinel	Monticellite	Clinopyroxene	Glass	Spinel	Clinopyroxene	Glass	Spinel	Glass
SiO ₂	53.29	1.22	33.87	41.29	48.58	0.28	41.39	47.94		
TiO ₂	0.00	1.25	0.00	1.35	0.65	1.28	1.35	0.00		
Al ₂ O ₃	24.47	13.19	0.00	16.04	21.73	14.49	15.90	16.48		
Cr ₂ O ₃	0.00	0.96	0.25	0.00	0.28	1.99	0.00	0.00		
FeO	5.41	55.54	26.15	9.15	10.59	57.85	9.22	19.05		
MgO	0.14	1.16	8.74	7.53	0.25	2.28	7.37	0.00		
MnO	0.00	0.00	0.31	0.00	0.18	0.00	0.00	0.26		
NiO	0.00	19.37	0.00	0.00	0.00	18.53	0.00	0.00		
CoO	0.00	2.98	1.31	0.53	0.00	3.05	0.53	0.66		
CaO	5.31	0.00	28.21	23.59	7.92	0.00	23.59	6.23		
Na ₂ O	7.34	0.00	0.00	0.22	5.24	0.00	0.22	3.13		
K ₂ O	3.18	0.00	0.00	0.00	3.49	0.00	0.00	4.51		
Total	99.14	95.67	98.84	99.70	98.91	99.75	99.57	98.26		
Component	zone 4					zone 5				
	Spinel	Clinopyroxene	Bunsenite	Glass	Bunsenite	Spinel	Olivine	Clinopyroxene	Glass	Spinel
SiO ₂	1.05	43.73	0.00	56.23	0.00	0.00	33.21	42.27		
TiO ₂	0.78	0.25	0.00	0.00	0.00	0.37	0.00	0.00		
Al ₂ O ₃	30.99	8.88	0.00	21.20	0.00	27.04	0.00	10.02		
Cr ₂ O ₃	6.88	0.00	0.00	0.00	0.00	4.44	0.00	0.00		
FeO	30.93	14.86	36.94	7.85	30.69	40.38	19.01	16.73		
MgO	4.61	5.21	2.31	0.00	3.43	2.93	16.60	3.53		
MnO	0.00	0.20	0.00	0.00	0.00	0.00	0.00	0.00		
NiO	20.51	3.18	54.21	0.44	59.59	22.75	27.80	3.74		
CoO	2.47	1.44	6.41	0.28	6.38	2.19	3.30	1.35		
CaO	0.00	21.98	0.00	3.91	0.00	0.00	0.00	22.02		
Na ₂ O	0.00	0.00	0.00	3.27	0.00	0.00	0.00	0.00		
K ₂ O	0.00	0.00	0.00	6.70	0.00	0.00	0.00	0.00		
Total	98.22	99.73	99.87	99.68	100.09	100.10	99.92	99.66		

zones 4 and 5 are Ni aluminomagnetite and trevorite. An analogous compositional trend was detected from the cores of the crystals to their outer zones. The compositional trends of the spinel are thus qualitatively similar for its populations I and II for both the zones of the column and the zones of the crystals themselves. The content of Mg in population-I spinel decreases from zone 0 to zone 4 from 1.1 to 0.7 a.p.f.u., and the analogous values for population II from zone 2 to zone 5 are 1.0 to 0.08 a.p.f.u. The Cr concentrations decreases from 0.7 to 0.5 a.p.f.u. for population I and from 0.4 to 0.0 a.p.f.u. for population II, while the Fe concentration increases from 0.02 to 0.5 a.p.f.u. (I) and from 0.3 to 1.7 a.p.f.u. The Al concentration also increases: 0.4–0.6 (I) and 1.1–1.3 (II). The differences in the latter instance are more significant, as is seen in the proportions of isomorphous Cr and Al (Fig. 8) or Fe and Mg.

There are many reasons for the differences in the composition of the spinel (and other minerals). These differences for the mineral of the earlier stage were caused by the addition or removal of components through the column, and the zoning of the crystals was formed due to uncompleted replacement reactions at zone boundaries. The general evolutionary tendency of the composition of spinel of population II reflects the changes in concentrations of components along the diffusion-controlled profile. When the mineral crystallizes from melt, its zoning is controlled by the incongruent character of crystallization.

The crystal chemical formulas of the spinel conventionally calculated with normalizing to three cations (Table 4) and four oxygen ions (this was possible because the mineral was analyzed for oxygen) do not differ within the errors of microprobe analysis. This provides us with sound grounds to conclude that the stoichiometric proportions of the cations to oxygen do not deviate from 3/4. This, in turn, allowed us to use the charge balance to calculate the degree of Fe oxidation Fe^{3+}/Fe_{tot} . According to this parameter, the spinel of population II is characterized by a higher degree of Fe oxidation: 0.7 on average. For this mineral of population I, the degree of Fe oxidation tends to decrease toward rear zones. The absence of this tendency in the frontal zones (as well as zones 1 and 2) is explained by the low Fe# of the spinel, because of which the degree of Fe oxidation is determined not as accurate. Conceivably, the tendency is explained by the reducing effect of the heater of the furnace and, hence, a gradient in oxygen fugacity across the zoning.

Judging from its morphology, spinel in the slag crystallized from melt, but its composition corresponds to Ni-bearing aluminoferrochromite, and this mineral differs from that of population I in that its Fe^{2+} dominates over Mg.

The monticellite of population I fills the intergranular space between periclase and spinel in zones 0 and 1. The mineral contains no more than 0.05 a.p.f.u. Fe and does not contain either Ni or Co. Monticellite in zones

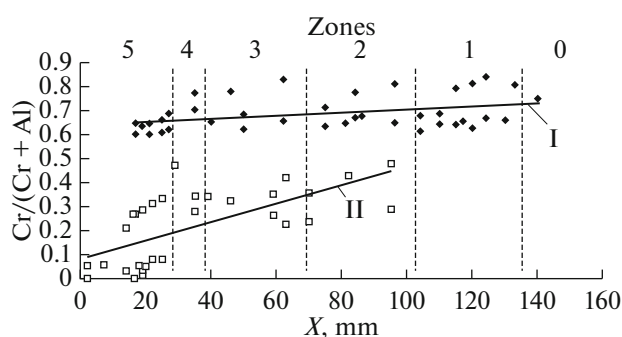


Fig. 8. Systematic variations in the atomic Cr/(Cr + Al) ratio of the spinel of populations I and II across reaction zones in a sample of refractory material.

2, 3, and 4 belongs to the later population and occurs as euhedral zoned crystals in glass (Fig. 4). Their cores contain 0.32 a.p.f.u. Fe, and the outer zones consist of Ni-bearing kirschsteinite with 0.65 a.p.f.u. Fe and up to 0.27 a.p.f.u. Ni. The monticellite is characterized by excess total Mg + Fe + Ni (1.05–1.15 a.p.f.u.) and corresponding deficit in Ca (0.80–0.95 a.p.f.u.).

The olivine of population I (zones 1 and 2) typically occurs as anhedral grains of magnesian composition, which are constrained to intergranular space between other minerals. From zone 1 to zone 2, the olivine systematically enriches in Fe (from 0.03 to 0.20 a.p.f.u.) and Ni (from 0 to 0.35 a.p.f.u.) and depletes in Mg (1.90–1.40 a.p.f.u.) and Ca (0.13–0.01 a.p.f.u.), and simultaneously it acquires trace concentrations of Co and Mn. In zones 2–5, elongate skeletal zoned crystals in glass were formed (Fig. 4). Their composition is almost constant: $Mg_{0.8}Fe_{0.4}Ni_{0.6}Co_{0.1}SiO_4$, with the Fe and Ni concentrations slightly increasing in the rims.

Clinopyroxene was found in reaction zones 2–5 and in the slag. This mineral always forms prismatic skeletal crystals in glass. In rear zones 4 and 5, the crystals are mostly $400 \times 30 \mu m$, i.e., one order of magnitude larger than in frontal zones 2 and 3. The mineral in the rear zones is richer in Fe and Al and contains Ni and Co. The differences are not caused by the zoning of the crystals, which is very insignificant. The slag hosts skeletal crystals $10\text{--}20 \mu m$, which resemble plant leaves. They are noted for low Ca concentrations: 0.4 a.p.f.u. All of the studied compositions are typical of metastable synthetic clinopyroxene that crystallize at rapid cooling.

The glass and mineral inclusions of population II in it were found in zones 2–5 and slag. The content of glass increases from zone 2 to zone 5. Olivine and monticellite are more typical of the frontal zones, while clinopyroxene and bunsenite are commonly found in rear zones, and spinel in distribution more evenly. The composition of the glasses corresponds to Fe-rich (and almost Mg-free) highly alkaline trachybasalt (wt %): 51.2 ± 3.1 ; $Na_2O 3.9 \pm 0.6$; $K_2O 5.3 \pm 1.2$ (Table 1).

Table 4. Crystal chemical formulas of spinel, calculated by normalizing to 3 cations, and degree of Fe oxidation in the mineral (calculated from analyses in Tables 2 and 3)

Component	Population I					Population II			
	0*	1	2	3	4	2	3	4	5
Si	0.00	0.00	0.00	0.00	0.00	0.04	0.01	0.03	0.00
Ti	0.00	0.00	0.00	0.01	0.01	0.03	0.03	0.02	0.01
Al	0.44	0.75	0.64	0.65	0.70	0.57	0.59	1.18	1.04
Cr	1.18	1.26	1.28	1.22	1.26	0.03	0.05	0.18	0.11
Fe _{tot}	0.53	0.22	0.19	0.21	0.61	1.69	1.68	0.84	1.10
Mg	0.85	0.77	0.88	0.92	0.43	0.06	0.12	0.22	0.14
Mn	0.00	0.00	0.00	0.00	0.00	0.00	0.00	0.00	0.00
Ni	0.00	0.00	0.00	0.00	0.00	0.57	0.52	0.53	0.60
Co	0.00	0.00	0.00	0.00	0.00	0.00	0.00	0.00	0.00
Fe ³⁺	0.38	0.00	0.07	0.12	0.03	1.25	1.27	0.54	0.83
Fe ³⁺ /Fe _{tot}	0.72	0.00	0.38	0.59	0.05	0.74	0.76	0.64	0.75
Fe ²⁺	0.15	0.23	0.12	0.09	0.58	0.45	0.41	0.30	0.27
Fe ²⁺ /(Fe ²⁺ + Mg)	0.15	0.23	0.12	0.09	0.58	0.88	0.78	0.57	0.66

* Zones.

DISCUSSION

Estimation of the glass composition. The fact that the altered part of the refractory material contains glass indicates that melt was involved in the reaction zones, but the compositions of the melt and quench glass produced by it are different because quench phases crystallized from this melt. The composition of melt was independently calculated for each zone by two different methods from analyses of the zones of the column (Tables 1 and 2) and the quantitative phase composition of the zones and quench phase aggregates, which were estimated from BSE images. In both instances, the calculations were conducted for a constant (50) number of oxygen ions, similar to broadly known T. Barth's method (Tables 5, 6), which is successfully applied in studying metasomatic processes. In applying the former technique, the concentrations of a cation in each mineral of a given zone were subtracted from the bulk-rock concentration of a cation (thereby only minerals of population I were taken into account, which were formed by reaction interaction), and then the difference was divided by the fractions of the minerals. For example, for Mg in zone of population II $(25.35 - 37.88 \times 0.53 - 9.90 \times 0.18 - 22.94 \times 0.15)/0.14 = 0.31$. The composition of melt in zone 5 is equal to the bulk composition because the zone contains only quench crystalline phases.

In the latter method, the concentration of a cation in the melt is equal to the total of its concentrations in each of the quench phases multiplied by the fractions of these phases. For Mg in zone of population II, $0.06 \times 0.30 + 0.92 \times 0.18 + 0.29 \times 0.05 + 4.26 \times 0.47 = 2.5$.

Upon recalculating all cations into oxides and normalizing to 100%, we obtained the composition of melt in the zone estimated by the two methods (Table 6, intermediate calculations are omitted). The maximum deviation from the average is 4.5 wt %, which is sometimes equal to 100 rel %. The poorest consistency between the estimates by the two methods was obtained for MnO and Cr₂O₃, and the best ones was for SiO₂ and FeO: less than 10 rel %. These values for other components vary within 25 rel %. The main sources of the errors are estimates of the volume fractions of phases and the attribution of individual grains to certain populations. The application of the more rigorous calculation method, with the use of the volumes, does not yield better results because involves additional errors stemming from the estimates of the volumes of phases of variable composition.

The column of transformations of the refractory material (Table 7). Being aware of all disadvantages of the calculations of the melt composition, we nevertheless managed to obtain fairly consistent results (Tables 1 and 5). The estimated compositions are the closest to those of natural melilitite (wt %): SiO₂ 35–40; (Na₂O + K₂O) 0.8–2.5 and differ from those of picrite and alkaline picrite in containing more Al₂O₃ and FeO at lower concentrations of MgO. The compositions systematically vary across the column toward the slag, whose composition is the closest to pyroxenite: 44 wt % SiO₂ and 2 wt % (Na₂O + K₂O).

Reactions at the boundaries of zones in the column of material addition and removal were calculated using formulas of population-I minerals and melt normalized to 50 oxygen ions, which makes the ratios of their

Table 5. Composition (wt %) calculated by normalizing to 50 oxygen ions, two methods for zones 2–5 of the column of altered refractory material at nickel-making in electric furnaces

Element	Calculation 1*						Calculation 2*					
	zone 2** (1)	periclase (0.53)	spinel (0.18)	olivine (0.15)	melt after 1* (0.14)	glass (0.30)	Spinel (0.18)	monticellite (0.05)	clinopyroxene (0.47)	melt after 2* (1)	melt, average	
Si	3.64	0.00	0.00	12.33	12.80	16.29	0.64	16.24	15.58	13.14	12.97	
Ti	0.01	0.00	0.03	0.00	0.06	0.00	0.50	0.00	0.38	0.27	0.16	
Al	3.08	1.00	6.70	0.10	9.49	8.80	8.20	0.00	7.12	7.46	8.48	
Cr	2.93	0.50	13.74	0.02	1.38	0.00	0.40	0.09	0.00	0.08	0.73	
Fe	6.04	6.91	8.14	1.40	5.04	1.38	24.45	10.45	2.88	6.69	5.87	
Mg	25.35	37.88	9.90	22.94	0.31	0.06	0.92	6.29	4.26	2.50	1.41	
Mn	0.08	0.00	0.10	0.06	0.36	0.00	0.00	0.13	0.00	0.01	0.18	
Ni	1.58	2.47	1.04	0.12	0.45	0.00	8.19	0.00	0.00	1.47	0.96	
Co	0.43	0.50	0.10	0.62	0.39	0.00	1.26	0.50	0.16	0.33	0.36	
Ca	0.34	0.00	0.01	0.62	1.74	1.74	0.00	14.50	9.54	5.73	3.73	
Na	0.23	0.00	0.00	0.00	1.64	4.34	0.00	0.00	0.16	1.38	1.51	
K	0.16	0.00	0.00	0.00	1.15	1.24	0.00	0.00	0.00	0.37	0.76	

Element	Calculation 1*						Calculation 2*					
	zone 3**	periclase (0.47)	spinel (0.23)	melt after 1* (0.30)	glass (0.35)	spinel (0.25)	clinopyroxene (0.4)	melt after 2* (1)	melt, average			
Si	4.19	0.18	0.00	13.68	15.83	0.14	15.65	13.25	13.46			
Ti	0.05	0.00	0.08	0.11	0.16	0.48	0.38	0.30	0.20			
Al	3.89	0.03	8.50	6.40	8.33	8.58	7.07	7.89	7.15			
Cr	2.90	0.04	12.41	0.10	0.07	0.79	0.00	0.16	0.13			
Fe	7.67	8.41	9.67	4.99	2.88	24.27	2.91	6.31	5.65			
Mg	21.19	39.50	8.80	2.02	0.12	1.72	4.18	1.92	1.97			
Mn	0.12	0.00	0.00	0.40	0.05	0.00	0.00	0.02	0.21			
Ni	1.70	1.26	0.00	3.70	0.00	7.46	0.00	1.19	2.45			
Co	0.40	0.38	0.00	0.74	0.00	1.23	0.16	0.26	0.50			
Ca	1.46	0.00	0.00	4.88	2.76	0.00	9.56	4.90	4.89			
Na	0.29	0.00	0.00	0.97	3.30	0.00	0.16	1.58	1.28			
K	0.20	0.00	0.00	0.68	1.45	0.00	0.00	0.67	0.67			

Table 5. (Contd.)

Element	Calculation 1*				Calculation 2*						melt, average	
	zone 4**	spinel	melt after 1*	glass	spinel	clinopyroxene	bunsenite	melt after 2*	bunsenite	clinopyroxene		melt after 2*
	(1)	(0.13)	(0.87)	(0.46)	(0.14)	(0.31)	(0.09)	(1)				
Si	11.00	0.00	12.64	16.25	0.45	17.14	0.00	12.85			12.85	12.75
Ti	0.13	0.08	0.14	0.00	0.25	0.07	0.00	0.06			0.06	0.10
Al	4.84	8.59	4.28	6.57	15.56	4.09	0.00	6.47			6.47	5.38
Cr	1.87	14.33	0.01	0.00	2.32	0.00	0.00	0.32			0.32	0.17
Fe	8.40	7.64	8.51	5.38	11.00	4.85	18.60	7.19			7.19	7.85
Mg	3.83	5.38	3.60	0.00	2.95	3.06	2.10	1.55			1.55	2.58
Mn	0.00	0.00	0.00	0.07	0.00	0.07	0.00	0.05			0.05	0.03
Ni	4.40	0.00	5.05	0.00	7.00	1.00	26.20	3.65			3.65	4.35
Co	0.60	0.00	0.69	0.18	0.84	0.45	3.10	0.62			0.62	0.66
Ca	1.95	0.00	2.24	2.26	0.00	9.23	0.00	3.90			3.90	3.07
Na	0.51	0.00	0.59	2.05	0.00	0.00	0.00	0.94			0.94	0.77
K	0.39	0.00	0.45	1.95	0.00	0.00	0.00	0.90			0.90	0.67
	Calculation 2*											
	Calculation 1*											
Element	zone 5 = melt (after 1*)	glass	spinel	olivine	clinopyroxene	bunsenite	melt after 2*					melt, average
	(1)	(0.27)	(0.17)	(0.09)	(0.36)	(0.07)	(1)					
Si	11.41	17.25	0.00	12.58	14.19	0.00	10.90					11.16
Ti	0.13	0.00	0.12	0.00	0.00	0.00	0.02					0.08
Al	5.04	7.65	13.62	0.00	3.94	0.00	5.95					5.50
Cr	0.65	0.00	1.50	0.00	0.00	0.00	0.26					0.45
Fe	8.76	2.01	14.38	6.00	4.69	15.31	6.54					7.65
Mg	3.86	0.00	1.88	9.42	1.77	3.06	2.14					3.00
Mn	0.00	0.00	0.00	0.00	0.00	0.00	0.00					0.00
Ni	4.56	0.11	7.78	8.42	1.00	28.57	4.84					4.70
Co	0.66	0.07	0.75	1.00	0.36	3.06	0.62					0.64
Ca	2.27	1.29	0.00	0.00	7.89	0.00	3.21					2.74
Na	0.66	1.95	0.00	0.00	0.00	0.00	0.57					0.61
K	0.42	2.63	0.00	0.00	0.00	0.00	0.76					0.59

* Melt compositions in zones of the column were calculated as follows: (1) by subtracting the compositions of minerals of population I, taken in their volumetric percentage in the zone, from the bulk composition of the zone and (2) by adding the compositions of the glass and minerals of population II with regard for the volumetric percentages of all phases. See text for details. ** Bulk composition of the zone. Values in parentheses denote volumetric percentages estimated from BSE images.

Table 6. Composition (wt %) of melt in discrete zones of the column of altered refractory material at nickel-making in electric furnaces

Oxides	Zone 2		Zone 3		Zone 4		Zone 5		Zone 00, slag
	average	deviation	average	deviation	average	deviation	average	deviation	
SiO ₂	36.11	1.76 (5)	35.67	0.01 (<1)	32.79	0.38 (1)	29.60	0.41 (1)	44.09
TiO ₂	0.59	0.35 (60)	0.71	0.35 (49)	0.33	0.13 (40)	0.26	0.19 (71)	0.75
Al ₂ O ₃	20.22	3.64 (18)	16.12	1.93 (12)	11.76	2.44 (21)	12.45	1.49 (12)	15.8
Cr ₂ O ₃	2.72	2.46 (91)	0.44	0.11 (24)	0.54	0.52 (96)	1.50	0.61 (41)	0.26
FeO	19.44	1.55 (8)	17.99	2.39 (13)	24.24	1.95 (8)	24.25	2.63 (11)	17.1
MgO	2.49	1.87 (75)	3.48	0.03 (1)	4.41	1.74 (39)	5.26	1.32 (25)	7.11
MnO	0.64	0.62 (97)	0.66	0.59 (89)	0.08	0.08(100)	0.00	0.00 (0)	0.29
NiO	3.24	1.58 (49)	8.05	4.03 (50)	13.98	2.21 (16)	15.63	1.04 (7)	0.99
CoO	1.26	0.19 (15)	1.65	0.78 (47)	2.11	0.11 (5)	2.12	0.02 (1)	1.02
CaO	9.39	4.59 (49)	12.10	0.22 (2)	7.38	2.02 (27)	6.85	1.42 (21)	9.68
Na ₂ O	2.19	0.33 (15)	1.76	0.44 (25)	1.02	0.24 (23)	0.84	0.03 (4)	1.02
K ₂ O	1.72	0.95 (56)	1.39	0.01 (1)	1.36	0.46 (34)	1.24	0.40 (32)	0.93

Averages are the averages of two calculation methods and deviations from the averages, wt %; values in parentheses are rel %.

molar amounts close to volumetric ratios. The actual phase proportions in each zone were compared with the ones calculated from the bulk compositions of the zones and the concentrations of inert components. The latter were selected from among SiO₂, Al₂O₃, MgO, FeO, Cr₂O₃, and CaO or the isomorphic components (Al₂O₃ + Cr₂O₃) and (MgO + FeO), which were regarded as a single component. For example, for frontal zones 1 and 2, the calculations (conducted with the MAPL computer program) of determinants with twelve combinations of the aforesaid components yielded absurd results in seven instances. The best consistence between the coefficients at phase formulas and the quantitative phase composition were obtained for SiO₂, (Al₂O₃ + Cr₂O₃), (MgO + FeO), and CaO. Analogous calculations were carried out for the other zones.

In the successive zones of the column, the major components MgO and Cr₂O₃ of the refractory material are systematically removed, while the slag components SiO₂, Al₂O₃, and FeO, as well as the components NiO and CoO of the metal melt, are simultaneously introduced. The input of components is less systematic for CaO and MnO. Obviously, components are removed into the supposed part of the slag adjacent to the refractory material; this zone is referred to as 01, but data on it are absent because the slag was tapped.

Other examples of corrosion of refractory materials by aggressive materials. The development of the zoning was modeled experimentally (Shchekina et al., 2014). Crucibles (made up of KhPTU refractory material, whose composition is similar to those of industrially used refractory materials) were charged with powdered industrial slag or with slag together

with metallic nickel. The samples were heated to a temperature of 1600°C and held for 12 h. At the contact between the refractory material and slag, five reaction zones developed (Fig. 9, shows zones 2–5), whose succession, phase composition, and the composition of each of the phases, as well as their evolution across the zoning, are almost identical to those described above. The total thickness of the column is 2–3 mm.

We have found (Gramenitskiy et al., 2005) a similar zoning in chromite–periclase refractory material that was affected by slag when NiS matte was obtained from oxide Ni ores in a horizontal converter vessel (at OJSC YUUNK, Orsk).

Reaction columns with zones containing melt are formed when slag interacts with Ankerhart SB25, TLS2, Jhearth 30BA, PPM-85 magnesian–dolomite masses (Shchekina et al., 2006a, 2006b; Gramenitskiy et al., 2008) in the floor of a Martin furnace in the process of steel-making at OJSC Omutninskii Metallurgical Plant, Vyksunskii Metallurgical Plant, and Chusovskoi Metallurgical Plant. The compositions of the reacting materials are principally different from those discussed above. As an illustrative example, below we consider the zoning in the hearth ramming of the Martin furnace with PPM-85 powder, produced by the Magnezit Company, Satka.

Upon the termination of the process, the cross section of the refractory material shows five clearly discernible zones. The most distant zone (zone 0) consists of fine-grained (0.2 mm) aggregates of periclase grains cemented by subordinate amounts of dicalcium silicate and perovskite. This zone is thought to be the sintered primary refractory material. The material of

Table 7. Inner structure of the corrosion column of refractory material (nickel-making in electric furnaces)

Zone	Inert components	Phases	Vol. fraction	Phase compositions and material balance at zone boundaries per 50 oxygen ions
0	(Mg,Fe)O	Periclase	0.68	Mg _{38.7} Fe _{3.5} Mn _{0.1}
	(Al,Cr) ₂ O ₃	Spinel	0.26	Mg _{11.2} Fe _{2.4} Cr _{16.2} Al _{8.1}
	SiO ₂	Olivine	0.06	Mg _{23.8} Fe _{0.8} Ca _{1.6} Si _{12.7} Mn _{0.1}
0 → 1		Addition Removal		1.4Si; 0.1Al; 0.6Ca; 0.1Na; 0.1Mn 0.1Cr; 2.9Mg
1	(Al,Cr) ₂ O ₃	Periclase	0.65	Mg _{40.0} Fe _{4.2} Mn _{0.1}
	(Mg,Fe)O	Spinel	0.18	Mg _{10.0} Fe _{2.8} Cr _{6.1} Al _{8.7}
	SiO ₂	Monticellite	0.10	Ca _{13.6} Mg _{17.3} Fe _{0.9} Mn _{0.1} Si _{15.9}
	CaO	Olivine	0.09	Mg _{23.9} Fe _{0.4} Ca _{1.2} Si _{12.7}
1 → 2		Addition Removal		1.5Si; 0.4Fe; 0.1Na; 0.2K 1.7Cr; 6.0Mg; 0.5Ca
2	(Al,Cr) ₂ O ₃	Periclase	0.53	Mg _{37.9} Fe _{6.9}
	(Mg,Fe)O	Spinel	0.18	Mg _{9.9} Fe _{8.1} Cr _{13.7} Al _{6.7} Mn _{0.1}
	SiO ₂	Olivine	0.15	Mg _{22.9} Fe _{1.4} Mn _{0.1} Ca _{0.6} Si _{12.3}
	CaO	Melt	0.14	Na _{1.0} K _{0.4} Ca _{3.7} Mg _{1.4} Fe _{5.8} Mn _{0.2} Ni _{1.0} Co _{0.4} Cr _{0.8} Al _{8.5} Si _{13.7}
2 → 3		Addition Removal		0.5Si; 0.8Al; 1.5Fe; 1.6Ni; 1.4Co; 1.1Ca; 0.1Na; 0.1K 4.2Mg;
3	(Al,Cr) ₂ O ₃	Periclase	0.47	Mg _{39.5} Fe _{8.4} Ni _{1.3} Co _{0.4}
	(Mg,Fe)O	Spinel	0.23	Mg _{8.8} Fe _{9.7} Cr _{12.4} Al _{8.5}
	SiO ₂	Melt	0.30	Na _{1.3} K _{0.7} Ca _{4.9} Mg _{2.0} Fe _{5.6} Mn _{0.2} Ni _{2.4} Co _{0.5} Cr _{0.1} Al _{7.2} Si _{13.5}
3 → 4		Addition Removal		6.8Si; 0.7Fe; 1.0Al; 2.7Ni; 0.2Co; 0.5Ca; 0.5Na; 0.2K 17.4Mg; 1.0Cr; 0.1Mn
4	(Al,Cr) ₂ O ₃	Spinel	0.13	Mg _{5.4} Fe _{7.6} Cr _{14.3} Al _{8.6}
	SiO ₂	Melt	0.87	Na _{0.8} K _{0.7} Ca _{3.1} Mg _{2.6} Fe _{7.8} Cr _{0.2} Ni _{4.4} Co _{0.7} Al _{5.4} Si _{12.8}
4 → 5		Addition Removal		0.4Si; 0.2Al; 0.4Fe; 2.7; 0.2Co; 0.3Ca; 0.2Na 0.1Mg; 1.2Cr
5	SiO ₂	Melt	1.00	Na _{0.6} K _{0.6} Ca _{2.7} Mg _{3.0} Fe _{7.6} Cr _{0.4} Ni _{4.7} Co _{0.6} Ti _{0.1} Al _{5.5} Si _{11.2}
00 Slag		Melt	1.00	Na _{0.7} K _{0.4} Ca _{3.6} Mg _{3.7} Fe _{4.9} Cr _{0.1} Mn _{0.1} Ni _{0.3} Co _{0.3} Ti _{0.2} Al _{6.4} Si _{15.1}

reaction zones 1 and 2 acquires a brecciated structure. Aggregates (0.5–1 mm) of periclase grains are cemented with fine-grained aggregates merwinite, Ti-bearing tricalcium aluminate, and dicalcium aluminate of blastic texture. The dicalcium silicate is replaced by merwinite and disappears at the contact between zones 1 and 2. In zone 3, small lenses appear that are made up of skeletal crystals of dicalcium silicate, brownmillerite, and a perovskite-like phase, which are cemented with merwinite. The texture of this material provides undeniable evidence that it was produced by quench crystallization of melt. According

to their composition, it plots within the liquidus region of the system CaO–Al₂O₃–SiO₂–TiO₂. In zone 4 (dark gray selvage in contact with melt), these aggregates are dominant. The rest of the material is small domains of recrystallized periclase, whose Fe# increases to 0.17–0.20. The changes in the chemical composition of the material across the column involve a systematic decrease in the Mg concentration and a simultaneous increase in the Ca, Si, Fe, and Al concentrations.

Glass-making systems are notably different from metallurgical ones. We have studied (Gramenitskiy and Batanova, 1996) the wear of KhATS-30 and

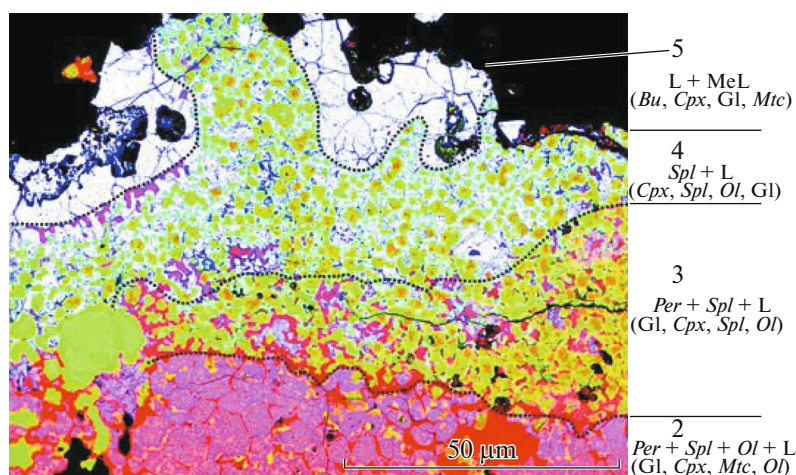


Fig. 9. Zoning in the region of reaction interaction between slag and refractory material. Cross section of a sample produced in an experiment on modeling the nickel-making process. Phase composition is indicated for the time when the zoning (melt + population I minerals) was formed. Phases formed during melt cooling are shown in parentheses (glass + population II minerals). BSE image.

Bakor-33 zirconium–aluminous refractory materials under the effect of molten alkaline glass. Across the zones, baddeleyite and the corundum [or the $(Al, Cr)_2O_3$] were the first to disappear, and simultaneously melt was generated and the compositions of the phases evolved. We will return to this example below when analyzing the evolution of the mineral compositions.

The transformations of refractory materials of various composition in contact with molten glass at temperatures of 1200–1500°C were documented in (Zigert, 1968) based on materials from the Lisichanskii Glass-Making Plant. The addition or removal of components control the origin of reaction zones, in which newly formed tridymite and cristobalite are found in the dinas; corundum, mullite, sodium aluminate, and nepheline occur in the aluminous refractory materials; and mullite, nepheline, carnegieite, albite, sodium aluminate, zircon, and baddeleyite develop in molted zirconium–aluminous refractory materials and, in all instances, in the glasses.

The aggressive material that affects the refractory materials is not only the molten silicate slag. Zoning of this type, with the origin of melt in the refractory materials was described by Fedorov et al. (2005) in refractory materials affected by Cu and Ni oxide melt (matte) during a certain stage of Cu production.

Reaction zones with newly formed silicate melt and alkaline aluminosilicates are produced when vapors affect chamotte refractory in the roof and stack of the blast furnace (Ivanov, 1954) and on the roof, suspended walls, torches, and other parts and facilities of glass melting furnaces (Zigert, 1968).

A similar zoning, with newly formed mullite, nepheline, hematite, and silicate melt was studied by

Malyshev et al. (2007) in the lining of a lime-regeneration furnace of the OJSC Arkhangelsk Paper Mill.

The origin of melt was detected by Zarskii (1989, p. 330) in the rear zone of alkaline metasomatism. Melt was also generated when pargasite was affected by NaCl-bearing aqueous fluid (Khodorevskaya and Aranovich, 2016). In these instances and the two described above, the systems originally did not contain melt at all.

We have detected the development of a number of reaction zones with newly formed aluminosilicate melt when olivine pyroxenite and dolerite were affected by hydrous granitic melt at 1150–1200°C (Gramenitskiy et al., 2001, 2002).

General characteristics of the zoning. The persistent presence of certain features of zoning produced in the course of so much different processes in compositionally different systems indicates that these features reflect certain common relations occurring when compositionally contrasting materials interact with one another.

(1) Zoning developing at the contacts shows systematic changes in the concentrations of components (their introduction or removal) in successive zones of the columns. In our basic example discussed in the section *Results* above, MgO and Cr_2O_3 are removed from the refractory material, as is reflected in the decrease in the contents of periclase and chromite and their replacement by phases poorer in these component and in the eventual disappearance of the minerals. Slag components (SiO_2 , FeO, and NiO) are transported in the opposite direction and produce phases with higher concentrations of these components. If the removal of components is not fully compensated, porosity and cavities are formed (chains of large pores along the boundaries of zones, first of all, between zones 3 and 4 in the basic example).

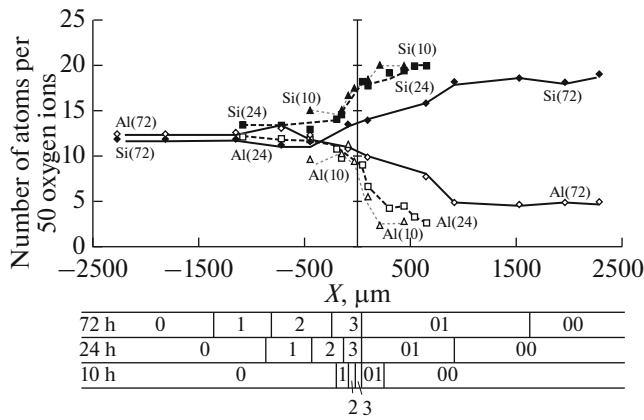


Fig. 10. Systematic variations in the Si and Al concentrations (numbers of atoms per 50 oxygen ions) in the glasses of reaction zoning modeled in experiments (10, 24, and 72 h) on imitating interaction between molten glass and baddeleyite–corundum refractory material. Distances in the cross section through the refractory material are indicated in micrometers from the original contact between the reaction materials (negative values correspond to the direction toward the refractory material, and positive ones toward molten glass). The positions of zones at various interaction time are shown at the bottom of the figure.

(2) New phases are formed only at zone boundaries, and this reflects changes in the chemical composition. Each zone differs from adjacent ones in the appearance and/or disappearance of a certain phase, and melt is generated at the boundary between zones 1 and 2 (in the basic example) and simultaneously monicellite disappears.

(3) The succession of the zones is always the same. For example, melt is never formed and periclase never disappears in the refractory material itself.

(4) Sharp contacts between zones are clearly seen both in hand-specimens (Fig. 2) and in petrographic thin sections (Figs. 4, 9) in the basic example above. The sharpness of the replacement fronts indicates that reaction rates at zone boundaries are higher than the rate of material transfer, i.e., local equilibrium is reached at any point in the column.

(5) The gradual changes in the compositions of the phases, as illustrated above by the examples of periclase (Fig. 7), spinel (Fig. 8), and olivine of population I across the zone succession, reflect the gradients of the chemical potentials and show that, as a rough approximation, equilibrium is reached inside of each zone.

These five features are illustrated by detailed description of the basic example above. Similarities with products of diffusion-controlled metasomatism are quite remarkable. However, the term *metasomatism* is inapplicable to this process: by definition, diffusion-controlled metasomatism is a replacement process, with the rock (material) necessarily preserving its

solid state. The most adequate and accurate definition in this instance is *melt* (or *magmatic* for natural processes) *replacement*.

Origin and growth of column zones. The development of the same succession of zones of various thickness in chromite–periclase refractory material during nickel-making led us to suggest that these zones start to develop simultaneously at the very beginning of the process and then proportionally increase in thickness. However, the above examples do not provide sufficient evidence in support of this hypothesis. These data were acquired (Gramenitskiy and Batanova, 1996) by means of experimental modeling of interaction between baddeleyite–corundum refractory material and melt in the process of glass-making. In addition to the inner structure of the column found in refractory material samples from industrial facilities, in modeling the glass-making process, we studied zones of the column of the primary reacting and contaminated melts.

In three experimental runs that lasted 10, 24, and 72 h at 1400°C, we obtained columns with identical successions of zones, their phase composition, and the composition of the phases (Fig. 10). This succession of zones (column) is as follows: 0. baddeleyite + corundum + mullite (primary refractory material). | 1. Baddeleyite + corundum + melt (n) | 2. baddeleyite + melt (n) | 3. melt (n) | 01. melt (c) | 00. melt (g), where the parenthetical characters *g*, *c*, and *n* denote three melt types quenched to glass: *g* for primary melt, from which the glass was made, *c* for same melt contaminated with components of the decomposed slag, and *n* for newly formed melt in reaction zones of the refractory material. Double bars indicate the original location of the boundary between reacting materials 0 and 00 (this boundary was marked in the experimental runs with a thin platinum wire). The location of the replacement fronts relative to this boundary (Fig. 10) in the experiments that lasted 10 h was as follows: (0 → 1) –165 μm, (1 → 2) –90 μm, (2 → 3) –30 μm, (01 ← 00) +200 μm. The values for the 24-h experimental run are –810, –450, –140, and +950 μm; and those for the 72-h run are –1420, –780, –250, and +1650 μm. As the duration of the experimental runs increased from 10 to 24 and 72 h, the distances of each of the four fronts correspond to the proportions 0.12/0.58/1, which are almost exactly proportional to the square roots of the respective experimental times, as follows from diffusion laws. These relations are valid starting at the moment of time when the process became stationary (likely in approximately 1 h). The thickness of the interaction zone is then 0.1–0.2 mm. In this understanding, it is reasonable to conclude that the zones of the column started to develop simultaneously and grew proportionally.

The role of melt. A feature typical of the columns, in contrast to metasomatic ones, is the occurrence of melt (glass) not only in the slag but also in the reaction

zones. In the refractory materials affected by metallurgical melts, the composition of the glass corresponds to that of the residual liquid left after the minerals of population II crystallized. In the last of the above examples (the process of glass-making), the samples were quenched and thus do not contain any minerals of population II, and the glass corresponds to the melt in composition.

In the cross section of the reaction region, concentrations of all components vary according to the concentration gradients (Fig. 10). As is typical of diffusion-controlled profiles, the concentration trajectories are S-shaped. With an increase in the duration of interaction, they tend to straighten like a bent flat spring. The growth rate of the zoning is consistent with the known diffusion coefficients of components in melts: 10^{-8} to 10^{-9} cm/s².

The origin of melt in the body of the altered refractory material should not be viewed as melting. This follows from the fact that the primary microtexture of the refractory material is inherited (together with the associated crystals of population II) when the glass is generated where now-decomposed minerals occurred. At the front of the most intense melt generation, spinel grains are corroded by vermicular glass veinlets 2–3 μm long (Fig. 5). The fact that the spinel grain retains its original shape proves that the glass veinlets were produced by means of replacement. An even more shining example is provided by the glass pseudomorphs after clinopyroxene ingrowths in an orthopyroxene grain (exsolution of the solid solution), which was described in experiments on interaction between granitic melt and olivine pyroxenites (Gramenitskiy et al., 2001).

It follows that melt was in situ generated in the reaction zones (as pseudomorphs are) and cannot by any means be understood as “impregnation by slag”, from which it differs in composition, the composition of the glass, and those of the minerals (Tables 1, 2).

Also, this melt could not be produced by partial “anatectic melting”, as follows from our experiments on interaction between granitic melt and dolerite (Gramenitskiy et al., 2002). According to the corresponding concentration gradients, the Ca# of the plagioclase and the Mg# of the pyroxene, and hence, the Ca/Na and Mg/Fe ratios of the glasses, decrease. In our blank experimental runs (without contact with granitic melt), partial melting produced reaction rims of calcic plagioclase and magnesian olivine and pyroxenes around primary dolerite minerals, i.e., the opposite (“restite”) compositional trends.

Melting is an isochemical process. At congruent melting, the composition of the primary solid phase or mixture of the starting phases corresponds to the composition of the melt, and if melting is incongruent, it is equal to the bulk composition of the newly formed phases and the melt. In the situations discussed above, no such correspondence of the compositions was detected. Melting is always initiated by a temperature

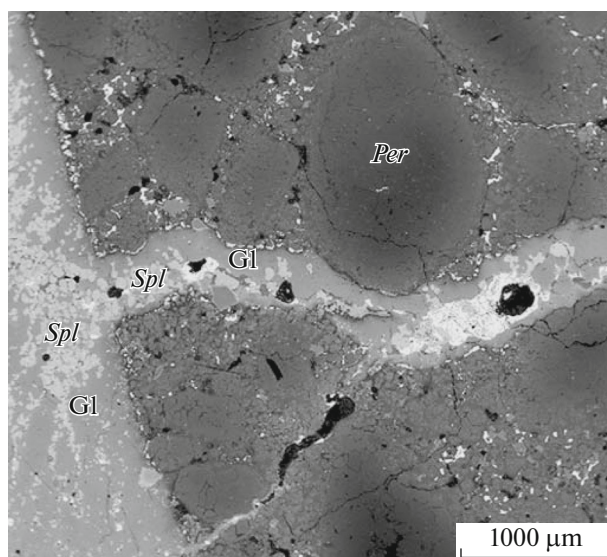


Fig. 11. BSE image of a crack that was filled with mush of melt and spinel crystals. The mush flew from the region of melt generation (zone of replacement with melt) through the crack that cut across metasomatic zones of the column. Converter processing nickel ores into nis material at YUUNK Co., Orsk.

increase. In industrial processes, temperature gradients do occur, of course, in the container walls and influence the intensity of corrosion. However, its main driving force is chemical interaction between the unequilibrated materials. Analogous results, with the development of reaction zoning, were obtained in isothermal experiments. The most adequate term for the origin of melt in such processes is *melt* (or for nature processes *magmatic*, according to D.S. Korzhinskii) *replacement*.

The newly formed melt can migrate/flow along fractures and cracks, as follows from our observations (Gramenitskiy et al., 2005) of the wear of refractory lining bricks of horizontal metallurgical converter furnaces when nickel matte is produced (during one of the processing stages of oxidized nickel ores). Together with spinel crystals, melt was forced off the zone where it was generated along fractures (Fig. 11) that cut across the metasomatic alteration zones and entering the unaltered refractory material. In the part of the refractory brick distant from the contact with slag and matte, the walls of the fracture (Fig. 12) are successively overgrown with olivine crystals and then by Fe-richer clinopyroxene and wüstite. The axial zones of the veinlets are made up of andesitic glass. The primary melts were never squeezed along fractures because they were separated from the refractory material by zones consisting of crystals and melt. No fractures cut across these zones, or at least, we have never noted such penetration of the primary melt.

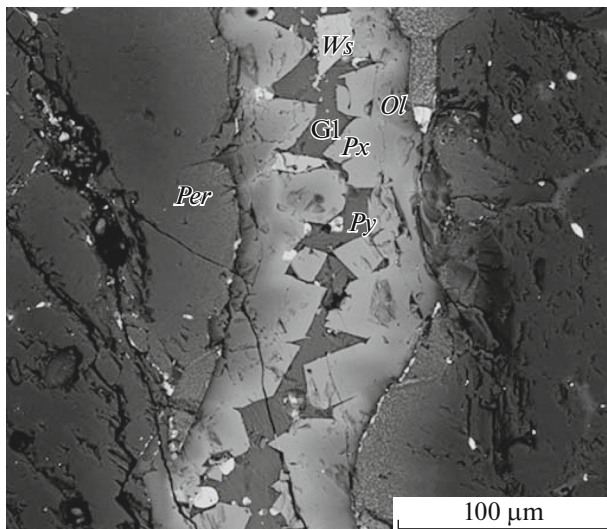


Fig. 12. BSE image of a crack filled with recrystallized melt that was forced off the melt replacement region into unaltered refractory material. Sample of refractory material used in the converter processing nickel ores into nis material at YUUNK Co., Orsk.

CONCLUSIONS: POSSIBLE IMPLICATIONS FOR GEOLOGICAL OBJECTS

The aforementioned features of the industrially generated columns, in whose zones crystalline refractory materials are replaced by melts, have certain unobvious implication of interest for studying naturally occurring magmatic replacement.

1. In rocks that are usually thought to be zones of metasomatic migmatization (“metasomatic preparation”) or adjacent to zones of contact metasomatic contamination of intrusions, melt inclusions can be found that were in equilibrium with crystalline phases (minerals) at the time of interaction. The groundmass of these rocks consists of host-rock minerals that were recrystallized (and their composition was thereby modified) and of minerals that crystallized from the melt. A single rock thus may show combinations of features produced by magmatic and metamorphic processes, similar to combinations of neo- and paleosome in migmatites.

2. Inasmuch as no melt is either preserved in magmatic-replacement zones in nature or quenched to glass, some of the minerals are found in two populations: the minerals of population I formed, together with melt, the column when it started to develop, while the minerals of population II crystallized from melt. They can be distinguished from one another based on their morphology, composition, and the zoning of their grains.

3. Replacement columns can be formed in which a number of zones consist of the same minerals and are separated from one another by sharp boundaries. At these boundaries, the proportions of the minerals

drastically change. For example, in the process of migmatization, plagioclase, quartz, and biotite are replaced by melt in the successive zones of the column. The same minerals of population II crystallize, together with potassic feldspar, from the melt. Consequently, the rear zones consist of two feldspars, quartz, and biotite.

4. Melt generation in metasomatic replacement zones explains the origin of ductile deformation features in these rocks. At the same time, brittle deformations are typical of the pristine rock and the frontal metasomatic zones of the column.

5. Unlike metasomatic columns, whose zone successions are always the same and each of the zones can be contacted exclusively by the neighboring one, the material of magmatic-replacement zones with melt can flow and be forced off its generation region along fractures into nearby metamorphic rocks, thereby intersecting outer (melt-free, metasomatic) zones.

Most of these features were found in the contact zone of the Syrostan granite massif (Gramenitskiy, 1990) before we started to study mechanisms destructing refractory materials. Now these features have received new interpretations.

ACKNOWLEDGMENTS

The authors thank Dr. E.V. Sokol (Sobolev Institute of Geology and Mineralogy, Siberian Branch, Russian Academy of Sciences) for constructive and benevolent criticism. We appreciate comments provided by the anonymous reviewers that led us to introduce additional materials into this publication and make it more understandable for the reader.

REFERENCES

- Fedorov, M.S., Ertseva, L.N., and Tsymbulov, L.B., Study of interaction of cinder with high concentrations of copper and nickel oxides with periclase, periclase–chromite, and chromite refractories, *Novye Ogneupory*, 2005, no. 8, pp. 41–47.
- Glossary of Geology*, Washington: Am. Geol. Inst., 2005.
- Gramenitskii, E.N., Mechanism of the magmatic replacement by the example of the contact zone of the Syrostan massif, South Urals, *Vestn. Mosk. Gos. Univ., Geol.*, 1990, no. 3, pp. 62–77.
- Gramenitskii, E.N., *Petrologiya metasomaticheskikh porod* (Petrology of Metasomatic Rocks), Moscow: INFRA-M, 2012.
- Gramenitskii, E.N. and Batanova, A.M., Regularities of interaction of refractory materials with glass-forming melts in light of the theory of diffusion-controlled zoning, *Steklo Keram.*, 1996, no. 8, pp. 9–13.
- Gramenitskii, E.N. and Lunin, P.V., Approaches to the experimental modeling of magmatic replacement, *Vestn. Mosk. Gos. Univ., Geol.*, 1996, no. 6, pp. 16–25.
- Gramenitskii, E.N., Shchekina, T.I., Batanova, A.M., et al., Formation of zoning during interaction of granitic

- melt with pyroxenite, *Vestn. Mosk. Gos. Univ., Geol.*, 2001, no. 3, pp. 27–37.
- Gramenitskii, E.N., Shchekina, T.I., Batanova, A.M., et al., Interaction of granitic melt with dolerite. Paper 2. Experiments at atmosphere pressure, *Byull. Mosk. O-va Ispyt. Prir., Otd. Geol.*, 2002, vol. 77, no. 5, pp. 77–84.
- Gramenitskii, E.N., Shchekina, T.I., Batanova, A.M., et al., Study of liquid phase chemical interaction of chromite–periclase refractory materials with aggressive media during obtaining of nickel nis matte in converter furnaces, *Novye Ogneupory*, 2005, no. 8, pp. 25–32.
- Gramenitskii, E.N., Batanova, A.M., Shchekina, T.I., et al., Mekhanizm iznosa periklazovogo materiala v podinakh martenovskikh pechei, *Novye Ogneupory*, 2008, no. 11, pp. 47–53.
- Ivanov, B.V., Decomposition of fire-clay lining of blast furnace by alkalis, *Ogneupory*, 1954, no. 3, pp. 121–127.
- Khodorevskaya, L.I. and Aranovich, L.Ya., Experimental study of amphibole interaction with H₂O–NaCl fluid at 900°C, 500 MPa: toward granulite facies melting and mass transfer, *Petrology*, 2016, vol. 24, no. 3, pp. 215–233.
- Khodorevskaya, L.I., Shmonov, V.M., and Zharikov, V.A., Granitization of amphibolites. 1. Results of first experiments with fluid filtering through rock, *Petrology*, 2003, vol. 11, no. 3, pp. 291–300.
- Korzhinskii, D.S., Granitization as magmatic replacement, *Izv. Akad. Nauk SSSR, Ser. Geol.*, 1952, no. 2, pp. 56–59.
- Korzhinskii, D.S., *Teoriya metasomaticheskoi zonal'nosti* (Theory of Metasomatic Zoning), Moscow: Nauka, 1982.
- Malyshev, I.P., Troyan, V.D., Troshenkov, N.A., et al., Application of MLS-62 refractory in lining of lime-generating rotary furnaces, *Novye Ogneupory*, 2007, no. 4, pp. 6–10.
- Shchekina, T.I., Gramenitskii, E.N., Batanova, A.M., et al., Application of magnesian–dolomite mass for furnace bottom of steel-making unit and study of mechanism of their deterioration during exploitation. 1. Study of Ankerhart refractories, *Novye Ogneupory*, 2006a, no. 10, pp. 45–54.
- Shchekina, T.I., Gramenitskii, E.N., Batanova, A.M., et al., Application of magnesian–dolomite mass for furnace bottom of steel-making unit and study of mechanism of their deterioration during exploitation. 2. Study of the Jehearth refractory mixture, *Novye Ogneupory*, 2006b, no. 12, pp. 31–41.
- Shchekina, T.I., Gramenitskii, E.N., Batanova, A.M., et al., Phase-forming processes and structural changes in chromite–periclase refractory materials applied for nickel production, *Novye Ogneupory*, 2011, no. 10, pp. 22–37.
- Shchekina, T.I., Batanova, A.M., Kurbyko, T.A., et al., Comparative study of the stability of chromite–periclase and periclase–carbonaceous refractories during their interaction with melts of nickel production (experimental data). 1. Behavior of chromite–periclase refractory materials in the presence of metallic slag and slag melts, *Novye Ogneupory*, 2014, no. 11, pp. 31–43.
- Zaraiskii, G.P., *Zonal'nost' i usloviya obrazovaniya metasomaticheskikh porod* (Zoning and Conditions of Formation of Metasomatic Rocks), Moscow: Nauka, 1989.
- Zharikov, V.A., Regime of components in melts and magmatic replacement, in *Problemy petrologii i geneticheskoi mineralogii* (Problems of Petrology and Genetic Mineralogy), Moscow: Nauka, 1969, vol. 1, pp. 62–79.
- Zigert, Kh., Petrographic study of refractories of glass-making furnace of the Lisichansk Glass Factory, *Extended Abstract of Cand. Sci. (Geol.-Min.) Dissertation*, Moscow: MGU, 1968.

Translated by E. Kurdyukov